Supplemental Data

ALS Mutation FUS-R521C Causes DNA Damage and RNA Splicing Defects

Haiyan Qiu, Sebum Lee, Yulei Shang, Wen-Yuan Wang, Kin Fai Au, Sherry Kamiya, Sami J. Barmada, Hansen Lui, Steven Finkbeiner, Caitlin E. Carlton, Amy A. Tang, Michael C. Oldham, Hejia Wang, James Shorter, Anthony J. Filiano, Erik D. Roberson, Warren G. Tourtellotte, Bin Chen, Li-Huei Tsai, Eric J. Huang

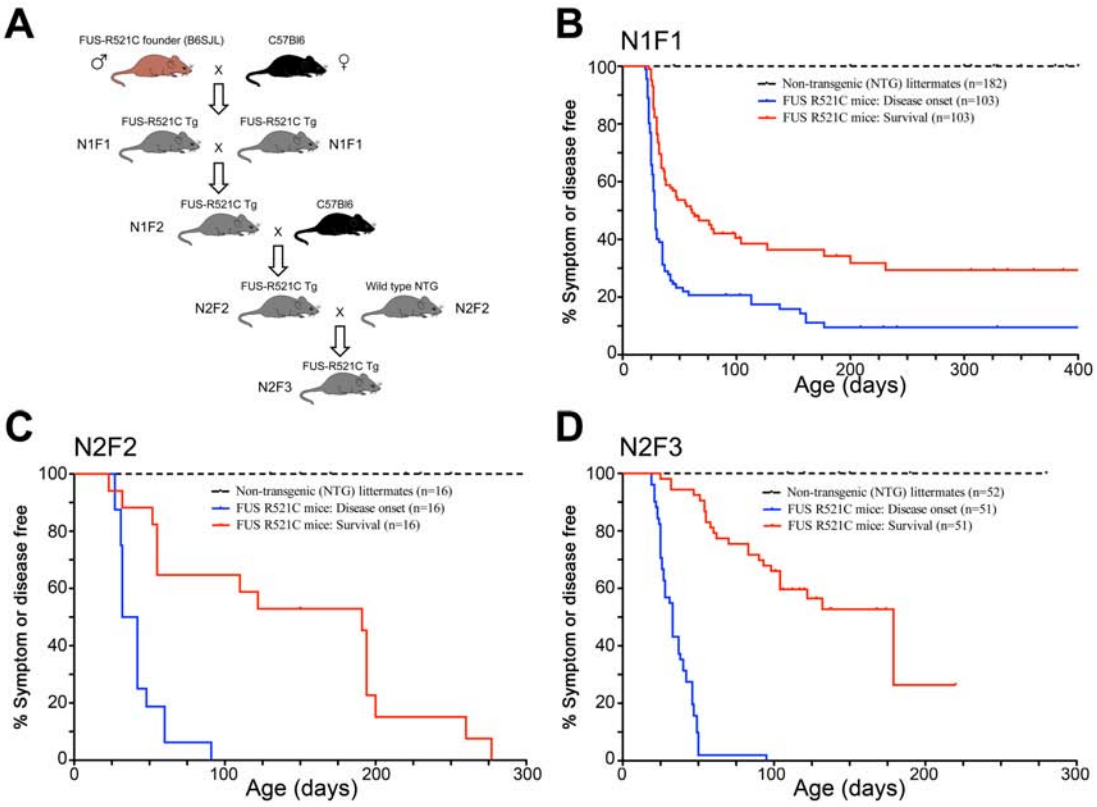

Supplemental Figure 1. Strategy to Propagate FUS-R521C Transgenic Mice and the Kaplan-Meir Curves for Disease Onset and Survival in N1F1, N2F2 and N2F3 FUS-R521C Mice.

(A) A schematic diagram showing the strategy to expand and propagate FUS-R521C transgenic mice from founders to N1F1, N2F2 and N2F3 generations. In brief, the FUS-R521C founder was mated with C57BL6 females to generate N1F1 mice. The surviving N1F1 mice (3-6 months old) are intercrossed to generate N1F2 mice, which were mated with C57BL6 to generate N2F2 mice. To maintain the FUS-R521C colony, N2F2 mice were intercrossed for N2F3 mice. (B) Kaplan-Meier survival curve for the disease onset and survival in N1F1 FUS-R521C mice (n=103) and non-transgenic littermate controls (n=182). (C-D) The disease onset and survival curves for N2F2 and N2F3 FUS-R521C mice were similar, supporting the successful propagation of the transgene and the reproducibility of FUS-R521C phenotype.

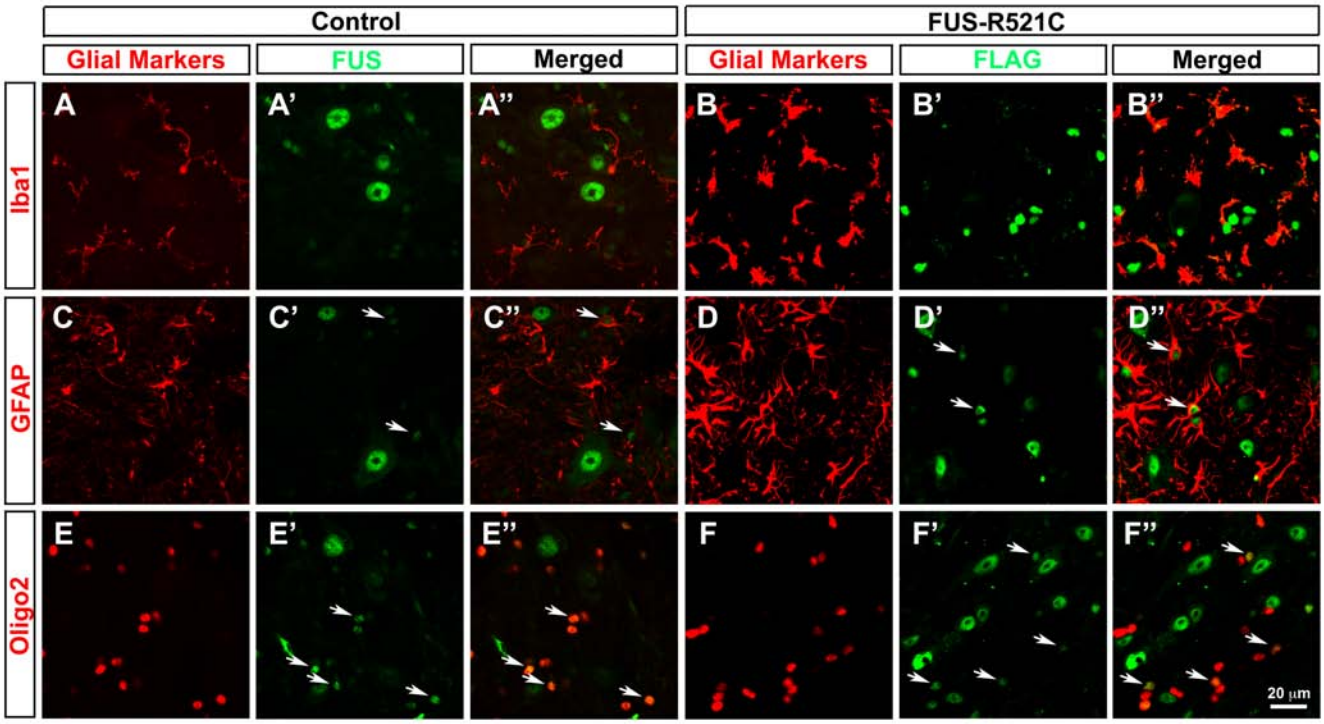

Supplemental Figure 2. Expression of the Endogenous FUS Proteins and FLAG-tagged FUS-R521C Transgenic Proteins in Glial Cells Within Spinal Cord.

(A-B'') Confocal microscopy shows no expression of FUS in Iba-1+ microglial in control spinal cord from wild type mice. Despite the presence of robust microgliosis, there is no detectable FLAG-tagged FUS-R521C transgenic protein in microglia of the spinal cord in FUS-R521C mice. (C-D'') Several GFAP-positive astrocytes (arrows) in control spinal cord express FUS proteins at levels lower than that in adjacent spinal motor neurons. Similarly, FLAG-tagged FUS-R521C proteins can be detected in several GFAP-positive astrocytes in the spinal cord of FUS-R521C mice (arrows). (E-F'') Similar to the results in astrocytes, both endogenous FUS and FLAG-tagged FUS-R521C proteins can be detected in Olig2-positive oligodendroglia in the spinal cord of control and FUS-R521C mice (arrows). Scale bar in panel F'' is 20 μm, and the same scale applies to all panels. Unlike the rabbit FUS polyclonal antibodies used in Figures 1 & 3, mouse monoclonal antibody for FUS cannot detect FUS in synapses or dendrites.

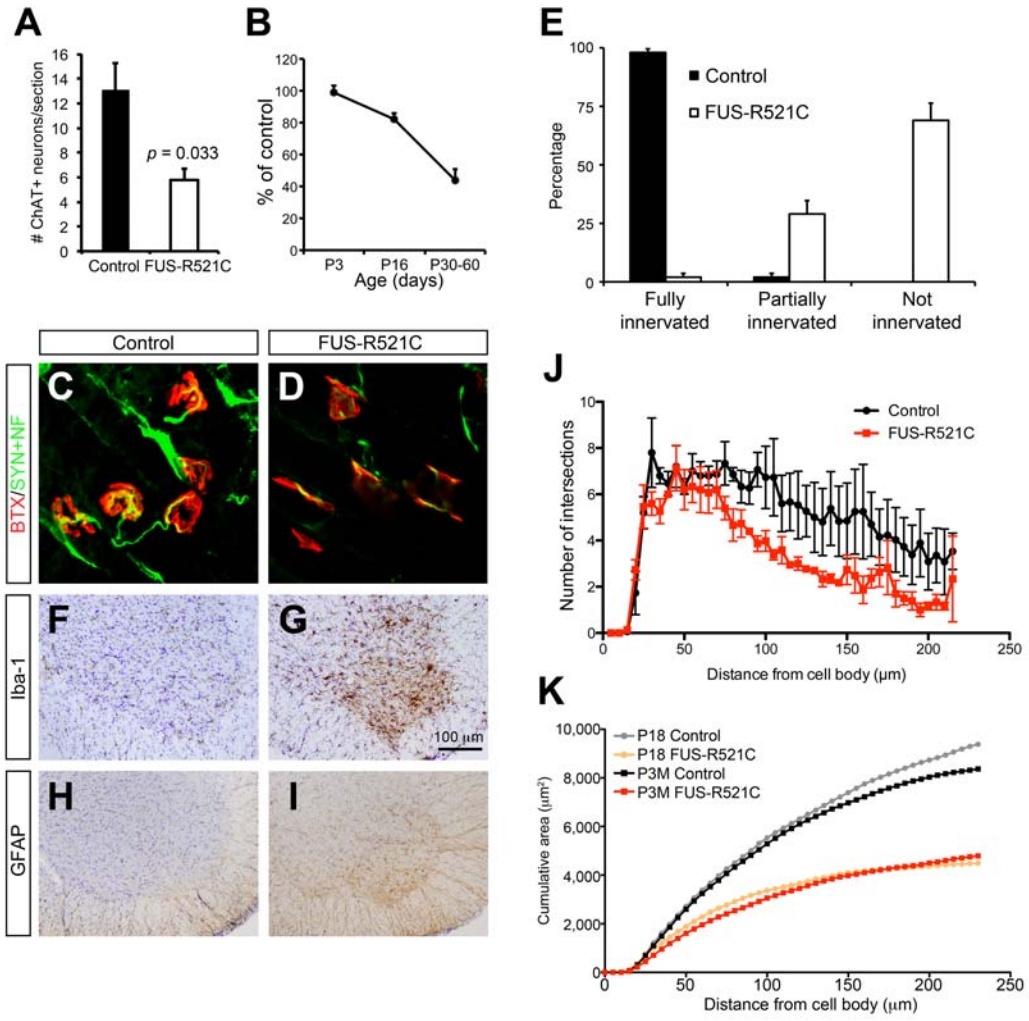

Supplemental Figure 3. Progressive Loss of Spinal Motor neurons and Deficits in the Innervation at the Neuromuscular Junction in FUS-R521C Transgenic Mice.

(A-B) Quantification of choline acetyltransferase (ChAT)-positive motor neurons in the cervical spinal cord of control and FUS-R521C transgenic mice at postnatal day (P) 3, P16 and P30-60 shows a progressive loss of motor neurons in FUS-R521C mice. By end stage (P30-60), there is ~55% loss of motor neurons in FUS-R521C mice. (C-E) FUS- R521C mice show defects in the innervation at the neuromuscular junction (NMJ). In contrast to the NMJ in non-transgenic controls, the majority of the NMJ in FUS-R521C mice are either not innervated or partially innervated (panel i). (F-I) Similar to the results in Supplemental Figure 3, the anterior horn of the spinal cord in FUS-R521C mice show a marked increase in microgliosis, highlighted by Iba1+ cells, and a very modest astrogliosis, shown by GFAP IHC. (J-K) Sholl analyses of dendritic branches and cumulative area of dendrites show that similar dendritic arborization defects in FUS-R521C spinal motor neurons can be detected in P18 mice.

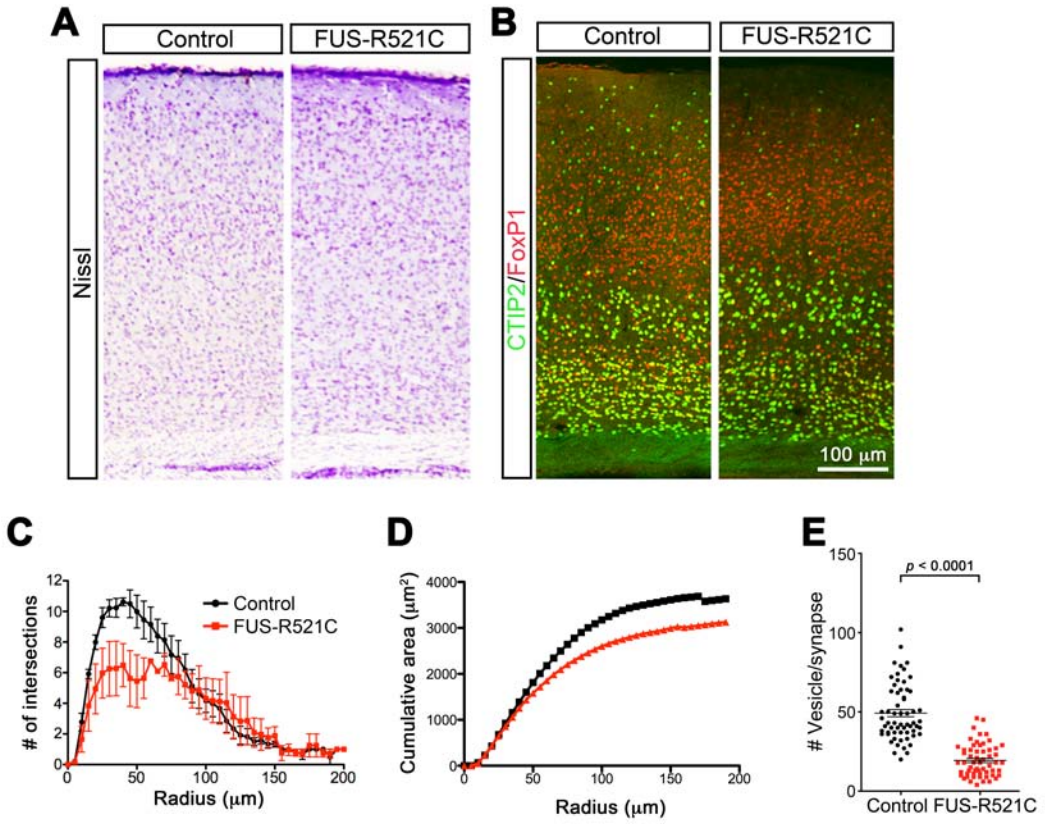

Supplemental Figure 4. Phenotype in the Basal Dendrites and Synapses in Layers IV and V of the Sensorimotor Cortex in FUS-R521C Mice.

(A-B) Nissl stains and layer-specific markers, CTIP2 and FoxP1, show no detectable differences in the general organization of the sensorimotor cortex in FUS-R521C transgenic mice. (C-D) Similar to the apical dendrites, the basal dendrites in layers IV and V of the sensorimotor cortex in FUS-R521C mice also show reduce branch points and reduced cumulative surface areas ($p < 0.0001$, 2-way repeated measures ANOVA). (E) Quantification of the number of synaptic vesicles per bouton shows significant reduction in the sensorimotor cortex of FUS-R521C mice ($p < 0.0001$, 2-tailed Student's *t* test, 54 high magnification [12,500x] fields from 3 control mice and 58 from 3 FUS- R521C mice).

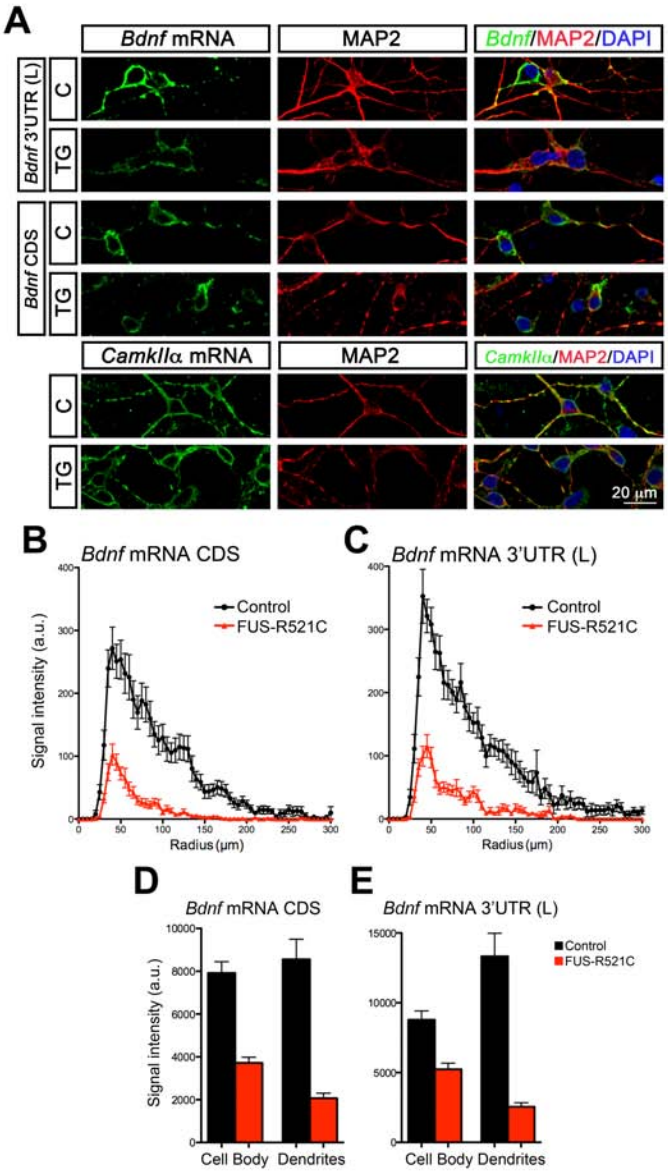

Supplemental Figure 5. Reduced *Bdnf* mRNA Expression in the Cell Body and Dendrites of Cultured Cortical Neurons from FUS-R521C mice.

(A) Cortical neurons cultured from E17.5 FUS-R521C embryos show reduced *Bdnf* mRNA in cell body and distal dendrites, whereas the expression and dendritic targeting of *CamkIIα* mRNA remains unchanged. (B-C) Neurolucida tracing and quantification of *Bdnf* mRNA fluorescent signal intensity, detected by *in situ* hybridization using either the probe that detects *Bdnf* coding sequence (CDS)(panel B) or 3' UTR long (L) sequence (panel C), shows consistent reduction of *Bdnf* mRNA in the cell body and along dendrites of cortical neurons from FUS-R521C transgenic mice. (D-E) Quantification shows significantly reduced total *Bdnf* mRNA signal in the cell body and dendrites of FUS-R521C-expressing neurons.

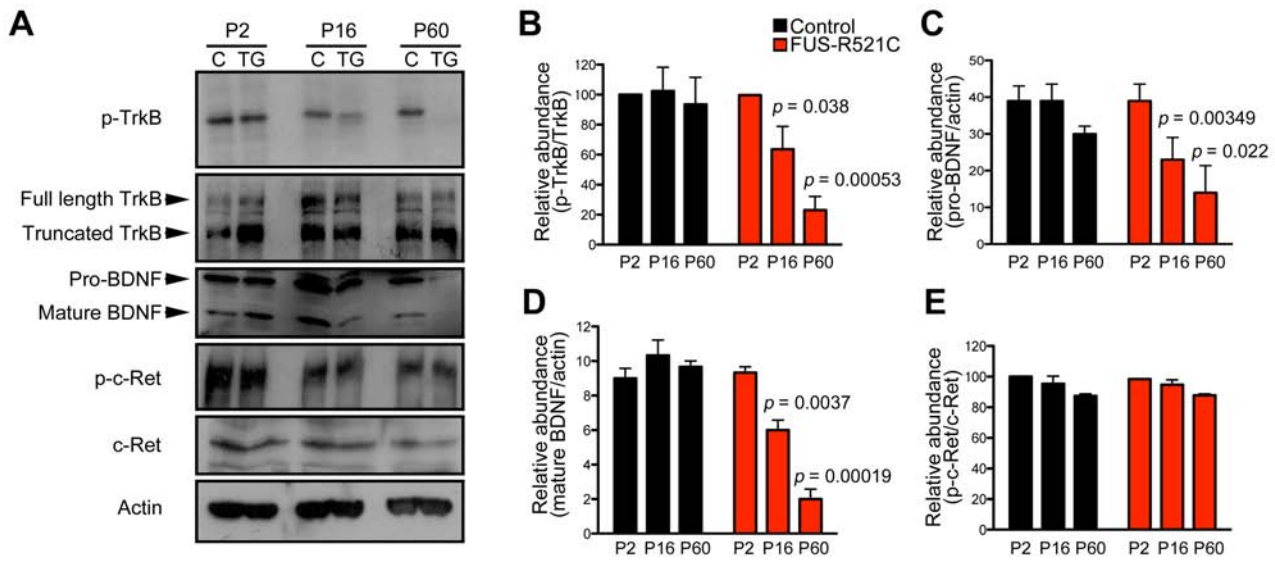

Supplemental Figure 6. Progressive Reduction in TrkB Activation and BDNF Protein Levels in the Spinal Cord of FUS-R521C Mice Without Affecting the Activation of GDNF Receptor c-Ret.

(A) Protein lysates are prepared from the spinal cord of control (C) and FUS-R521C (TG) mice at postnatal day 2 (P2), day 16 (P16) and day 60 (P60) to detect the relative abundance of activated TrkB receptor (detected using a phosphor-specific TrkB antibody), full length and truncated TrkB, pro-BDNF, mature BDNF, activated GDNF receptor c-Ret (p-c-Ret) and total c-Ret using Western blot analyses. The experiments are repeated using tissues from three control and FUS-R521C mice, and results are quantified using NIH ImageJ. (B-E) The relative abundance of activated TrkB receptor (p-TrkB), pro-BDNF and mature BDNF shows no detectable difference between control and FUS-R521C mice at P2, but a progressive reduction from P16 to P60 (panels C to D). In contrast, the level of activated c-Ret receptor shows no difference in the spinal cord of control and FUS-R521C mice (panel E). Statistics, Student's *t* test, n = 3 for each condition.

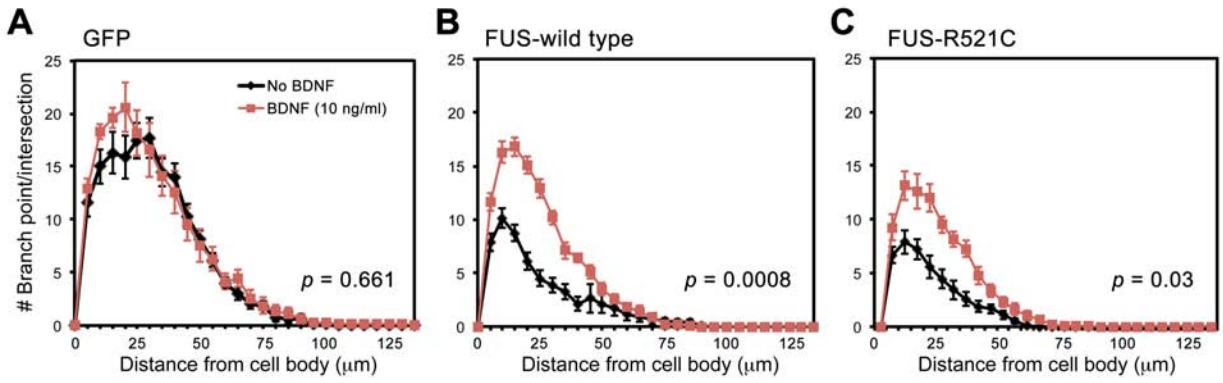

Supplemental Figure 7. Exogenous BDNF Partially Ameliorates the Dendritic Arborization Phenotype of Cortical Neurons expressing Wild Type FUS or FUS-R521C.

(A-C) Cortical neurons prepared from the cortices of E15.5 wild type embryos are transfected with plasmids expressing GFP, wild type FUS or FUS-R521C on day 7 after plating (7 DIV). The transfected neurons are then cultured for 7 days (7 DIV) in the absence or presence of recombinant BDNF (10ng/ml) before they are collected for immunostaining for TuJ1 antibody to highlight dendrite morphology. The dendrite morphology in transfected neurons is captured using Neurolucida tracings and the complexity of dendritic arborization is quantified using Sholl analyses. Significant dendritic growth retardation is also noted in neurons expressing wild type FUS (B) or FUS-R521C (C). Exogenous BDNF (10 ng/ml) partially ameliorates the dendritic growth phenotype in neurons expressing wild type FUS or FUS-R521C. At least 30 neurons are captured and quantified. Statistics uses 2-way repeated measures ANOVA.

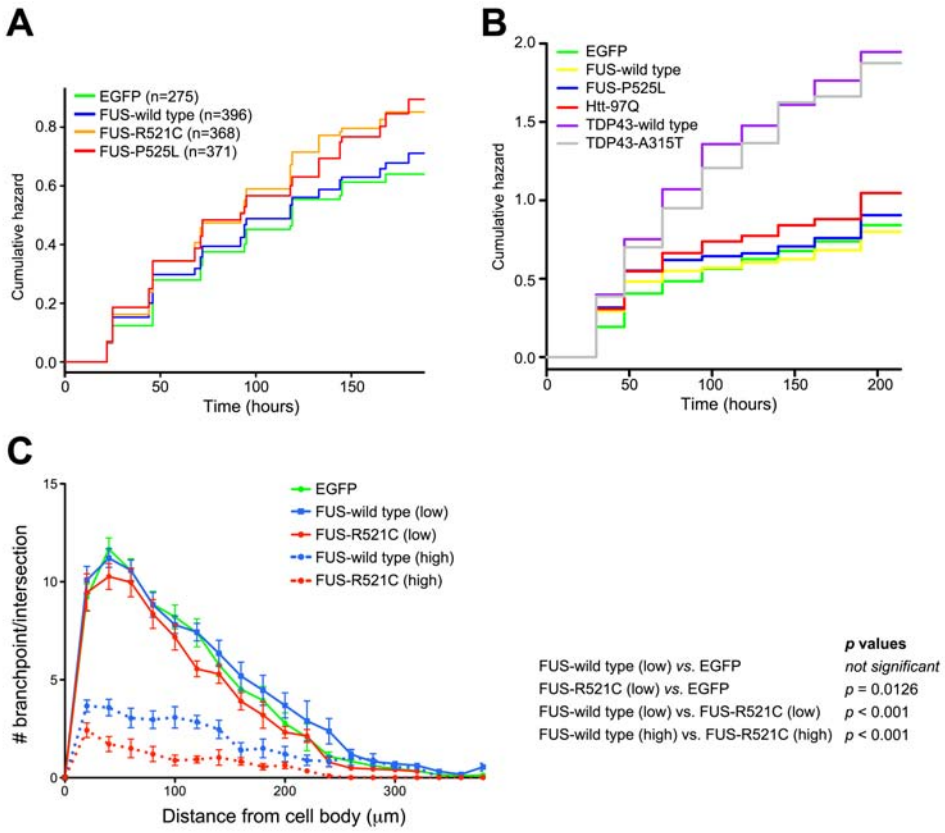

Supplemental Figure 8. Expression of Wild Type FUS or FALS-associated Mutation FUS-R521C or FUS-P525L in Cortical Neurons Leads to Modest Cell Death and Dose-Dependent Dendritic Defects.

(A) E15.5 wild type cortical neurons are transfected at 7 DIV with plasmids that expressed GFP, GFP-FUS wild type, GFP-FUS-R521C or GFP-P525L. Images of the transfected neurons are captured using automated microscopy to monitor the survival of hundreds of neurons over the course of 10 days. Using the previously established criteria for neuronal death, we showed that the cumulative hazard curves of neurons expressing wild type FUS showed no significant increase in the relative risk of cell death (HR: 1.08, $p = 0.624$). In contrast, the relative risk of cell death was higher in neurons expressing FUS-R521C or FUS-P525L (HR: 1.40, $p = 0.039$ for FUS-R521C and HR: 1.38, $p = 0.049$ for FUS-P525L). (B) The effects of FUS-R521C and FUS-P525L on neuronal survival appeared to dosage-dependent as lower FUS cDNA concentrations had less prominent toxicity to neurons. Intriguingly, however, compared to the same DNA concentrations of mutant huntingtin-97Q (Htt-97Q), wild type TDP43 or TDP43- A315T, expression of wild type or mutant FUS proteins led to lower cytotoxicity in cultured neurons. (C) Sholl analyses show dose-dependent reduction of dendritic arborization caused by wild type FUS and FUS-R521C. Side-by-side comparisons show that FUS-R521C mutant proteins consistently cause more severe dendritic defects in cortical neurons.

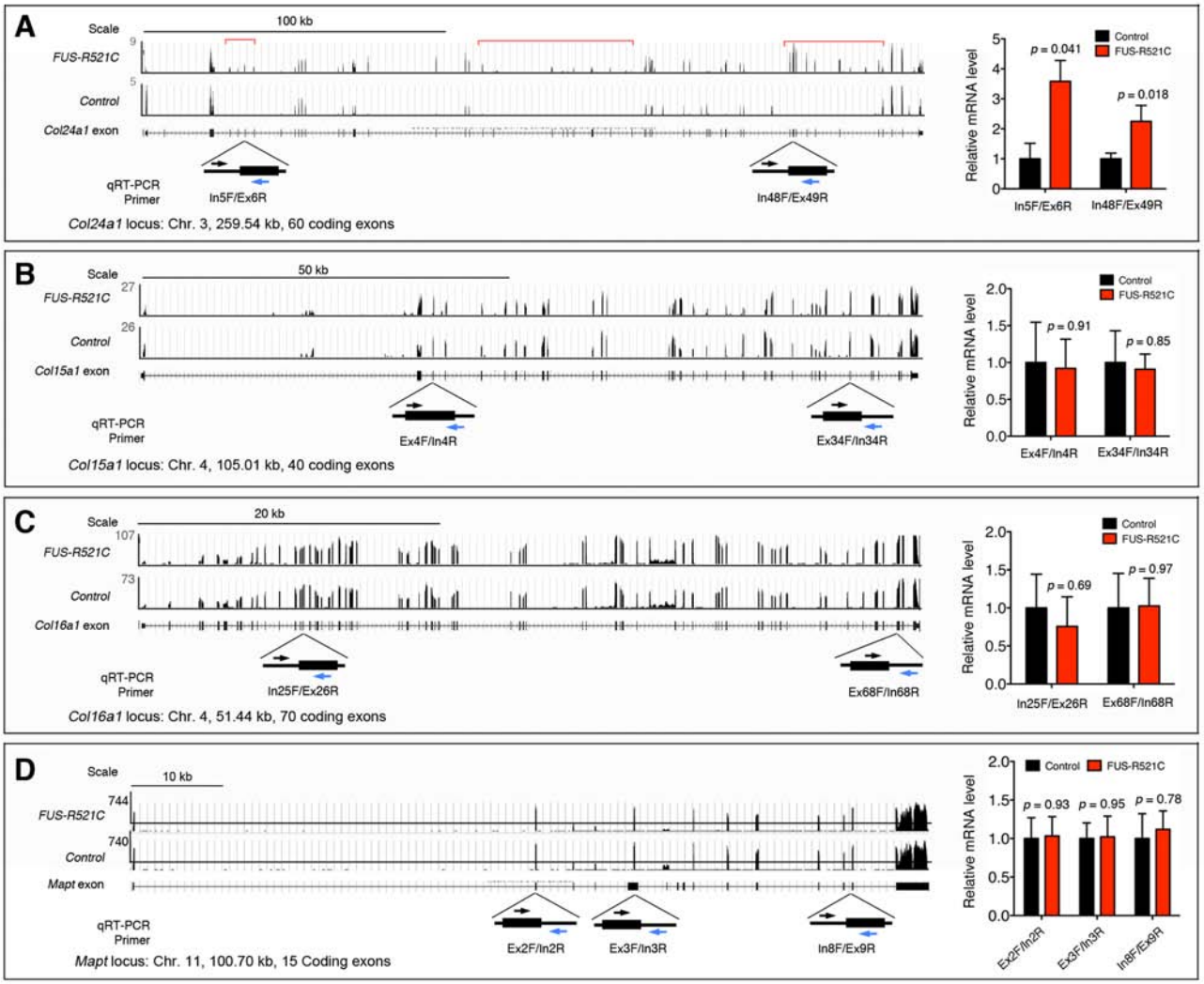

Supplemental Figure 9. RNA splicing defects in *Col24a1* gene, but not in *Col15a1*, *Col16a1* or *Mapt* (*tau*) genes.

(A) The mouse *Col24a1* gene is located on mouse chromosome 3 and encompasses ~259Kb with 60 exons. In FUS-R521C spinal cord, *Col24a1* mRNA shows evidence of excessive inclusion of cassette exons (highlighted by the bracketed regions). (B-D) In contrast, *Col15a1* (chromosome 4, 40 exons), *Col16a1* (chromosome 4, 70 exons) and *Mapt* (aka *tau*, chromosome 11, 15 exons) show no evidence of increase in exon inclusion or intron retention. RNA-seq data are further confirmed by qRT-PCR using primers that detect the presence of 5' and 3' splice junctions in *Col24a1, Col15a1, Col16a1* and *Mapt*. Quantifications of the qRT-PCR data are shown in each panel. Statistics uses Student's *t* test, n = 3.

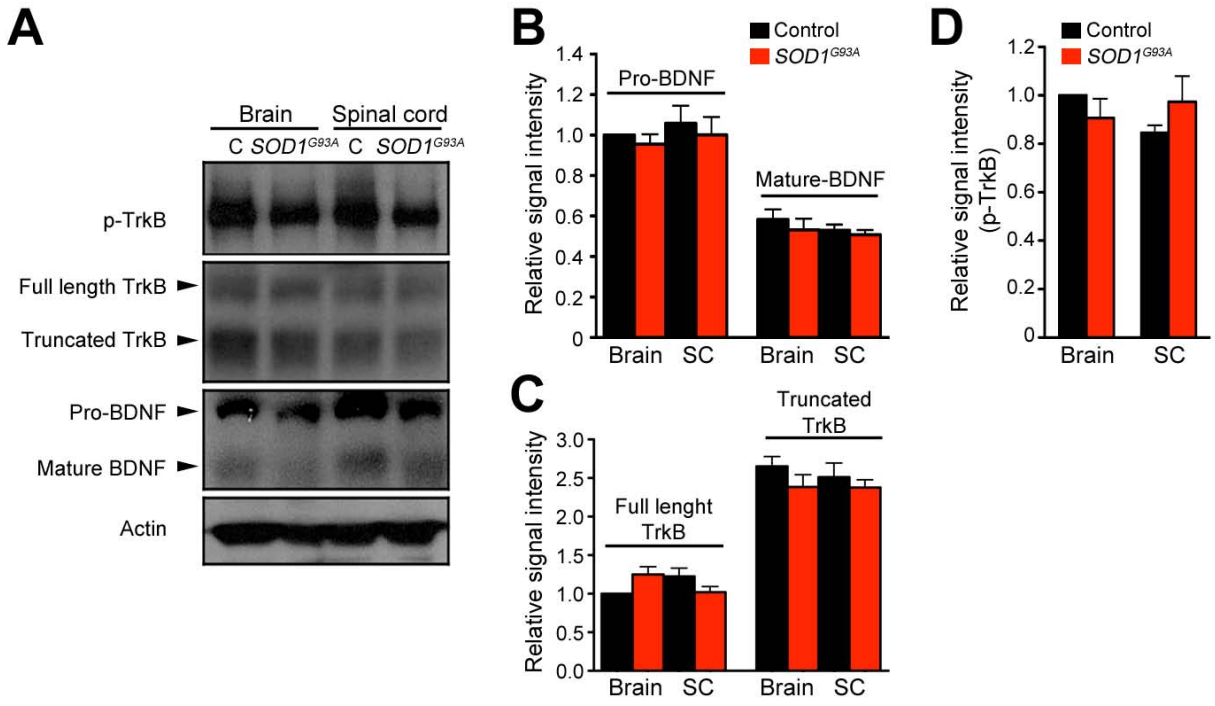

Supplementary Figure 10. No Detectable Reduction of BDNF Protein or TrkB Activation in the Spinal Cord Tissues of *SOD1^{G93A}* Mice.

(A) Western blot analyses show no detectable difference in the level of activated TrkB receptor (detected using a phosphor-specific TrkB antibody), full length and truncated TrkB, pro-BDNF and mature BDNF in protein lysates from the spinal cord of control (C) and *SOD1^{G93A}* mice at end-stage. The experiments are repeated using tissues from three control and FUS-R521C mice, and results are quantified using NIH ImageJ. (B-D) Quantification of the Western blot results shows no difference in the relative abundance of activated TrkB receptor (p-TrkB), full-length TrkB, truncated TrkB, pro-BDNF and mature BDNF between control and *SOD1^{G93A}* mice at end-stage,

Supplemental Table 1. DAVID Bioinformatics Gene Ontology (GO) Analyses of RNA-seq results from FUS-R521C spinal cord. (Related to Figure 8)

Genes With Increased Reads

Functional annotation	GO groups	Adjusted *p* value	Gene list
Extracellular matrix (Enrichment score 9.42)	GO:0005578 GO:0005581 GO:0005201 GO:0031012	2.01E-10 4.76E-10	*ADAMTS10, ADAMTS16, ANGPTL4, ANXA2, COL5A2, COL5A3, COL7A1, COL11A1, COL16A1, COL24A1, COL27A1, COL28A1, DCN, EMID2, ENTPD2, LAMA5, LGALS3, LOX, MATN2, MMP12, MMP19, OGN, POSTN, TGFBI, TIMP1, WNT10B, VWA1*
Lymphocyte mediated immunity (Enrichment score 7.13)	GO:0002449 GO:0019724 GO:0002250 GO:0002460 GO:0002443 GO:0016064 GO:0002252	1.44E-08 2.76E-08 4.61E-08 4.61E-08 8.92E-08 2.25E-07 6.27E-07	*BCL3, C1QA, C1QB, C1QC, C3, C4B, FCER1G, FCGR2B, FCGR3, ICAM1, ICOSL, IRF7, PTX3*
Enzyme inhibitor activity (Enrichment score 3.88)	GO:0004857 GO:0004866 GO:0030414	3.73E-05 1.70E-04 3.67E-04	*A2M, AGT, ANGPTL4, ANXA2, ANXA3, C3, C4B, CD109, CDKN1A, COL7A1, COL28A1, CST7, SERPINA3N, SPINT1, SPINT2, TIMP1*
Collagen (Enrichment score 3.82)	GO:0005581 GO:0005201	2.73E-05 0.001996204	*COL5A2, COL5A3, COL11A1, COL24A1, COL27A1, LOX*
Chemotaxis (Enrichment score 3.38)	GO:0042330 GO:0006935 GO:0007626	1.97E-04 1.97E-04 0.00522163	*C3AR1, CCL2, CCL3, CCL6, CCL11, CMTM3, CXCL10, FCER1G, FCGR3, HOXD9, HOXD10, IL16*
Proximal/distal pattern formation (Enrichment score 2.96)	GO:0009954 GO:0035113 GO:0030326 GO:0035107 GO:0035108 GO:0060173 GO:0048736	2.58E-07 0.002210077 0.002210077 0.005691661 0.005691661 0.006837974 0.006837974	*HOXA9, HOXA10, HOXA11, HOXC10, HOXC11, HOXD9, HOXD10, HOXD11*
Positive regulation of phagocytosis (Enrichment score 2.73)	GO:0050766 GO:0050764 GO:0045807 GO:0030100 GO:0051050 GO:0060627	5.50E-05 8.42E-05 3.85E-04 0.002739265 0.011758098 0.01926849	*C3, CARTPT, CLEC7A, FCER1G, FCGR2B, FCGR3, PTX3, TRIP6*
Anterior/posterior pattern formation (Enrichment score 2.47)	GO:0009952 GO:0003002 GO:0007389	1.36E-04 6.80E-04 0.002601203	*EGR2, HOXA9, HOXA10, HOXA11, HOXC9, HOXC10, HOXC11, HOXC13, HOXD9, HOXD10, HOXD11, OTX2, PCGF2, SOSTDC1*
Complement activation, classical pathway (Enrichment score 2.15)	GO:0002455 GO:0006958 GO:0006959 GO:0006956 GO:0002541 GO:0051605	4.42E-04 0.002197529 0.003234547 0.004329258 0.004329258 0.032815789	*BCL3, C1QA, C1QB, C1QC, C3, C4B, CLEC7A*
Chemokine activity (Enrichment score 1.98)	GO:0008009 GO:0042379	0.004801982 0.005275903	*CCL2, CCL3, CCL6, CCL11, CXCL10*

Genes With Decreased Reads

Functional annotation	GO groups	Adjusted *p* value	Gene list
Synapse (Enrichment score 8.99)	GO:0044456 GO:0045202	5.27E-10 1.62E-09	*ANKS1B, ARC, BSN, CHRM1, CHRM2, DLGAP2, GLRA1, GRID2, GRIN3A, GRIN2B, LZTS1, NRGN, PCLO, PSD3, RIMS1, SHANK2, SLC17A7, SV2C, SYT2*
Gated channel activity (Enrichment score 7.90)	GO:0022836 GO:0015267 GO:0022803	2.37E-09 3.97E-09 3.97E-09	*CACNA1E, CACNG2, CLCN5, GRID2, GRIN2A, GRIN2B, GRIN3A, GRIN3B, HCN2, KCNA2, KCNB2, KCNC3, KCNH3, KCNH7, KCNJ4, KCNJ6, KCNJ14, KCNK9,*

	GO:0046873 GO:0005261 GO:0005216 GO:0022838 GO:0030001 GO:0006812	4.38E-09 6.67E-09 7.22E-09 1.36E-08 2.74E-07 4.80E-06	*KCNMA1, RYR2*
Integral to membrane (Enrichment score 7.81)	GO:0016021 GO:0031224	2.56E-05 7.14E-05	*ANKS1B, BMPR2, CALN1, CHRM2, DCC, DHCR24, DNAJB14, ERBB4, HHIP, HTR2A, KCNG4, LDLR, MGAT5, PTK2B, RASL10A, SLC26A2, SPINK10, SUSD2, UGT8A, VIPR2 (total 140 genes)*
Voltage-gated cation channel activity (Enrichment score 7.04)	GO:0022843 GO:0005244 GO:0022832	1.02E-07 2.12E-07 2.12E-07	*CACNG2, CLCN5, HCN2, KCNMA1, KCNA2, KCNB2, KCNC3, KCNG1, KCNG4, KCNH3, KCNH7, KCNJ4, KCNJ6, KCNJ14, KCNK9, SCN8A*
Voltage-gated potassium channel activity (Enrichment score 6.55)	GO:0030955 GO:0031420 GO:0005267 GO:0006813 GO:0005249	2.71E-07 2.79E-07 7.67E-07 1.98E-06 2.10E-06	*HCN2, KCNA2, KCNB2, KCNC3, KCNG1, KCNG4, KCNH3, KCNH7, KCNJ4, KCNJ6, KCNJ14, KCNK9, KCNMA1, SLC5A7, SCN8A, SLC9A7, SLC10A4, SLC17A7*
Synaptic transmission (Enrichment score 6.06)	GO:0007268 GO:0019226 GO:0007267	2.52E-07 2.76E-07 9.78E-06	*ATXN1, CACNG2, CHAT, CHRM1, EGR3, GLRA1, GRID2, GRIN2A, GRIN2B, GRM3, KCNMA1, NCAN, PCLO, SHC3, SLC17A7, SLC5A7, STX1B, SV2C, UGT8A*
Sterol biosynthetic process (Enrichment score 5.80)	GO:0016126 GO:0016125 GO:0006694 GO:0008203 GO:0008202	5.82E-08 1.71E-06 6.99E-06 4.90E-05 2.37E-04	*CYP51, DHCR7, DHCR24, HMGCR, HMGCS1, HSD17B7, LDLR, LSS, MVD, SC4MOL, SC5D, SORL1*
Ion binding (Enrichment score 4.76)	GO:0043167 GO:0046872 GO:0043169	1.36E-05 1.61E-05 2.44E-05	*AOX4, ATP2A1, BMPR2, BSN, CALN1, CBL, CIT, FASN, GUCY1A2, KCNG1, KCNG4, KCNJ4, LDLR, MFAP4, NOS1, NR2E1, PCLO, RYR2, TESC, TRIM2, TRIM16 (total 105 genes)*
Neuron projection development (Enrichment score 4.60)	GO:0031175 GO:0048812 GO:0030030 GO:0048666 GO:0007409 GO:0030182 GO:0048858 GO:0048667 GO:0000904 GO:0032990 GO:0000902 GO:0032989	1.61E-07 6.09E-06 9.95E-06 1.07E-05 1.27E-05 2.22E-05 2.90E-05 4.11E-05 4.97E-05 4.97E-05 7.71E-04 0.00102235	*APC, CHAT, CIT, DCC, DST, EPHB1, FEZF2, FOXG1, GAS7, GRIN3A, LHX2, MNX1, MTAP1B, NEFL, NKX2-9, NR2E1, RTN4RL2, SEMA5A, TBR1*
Ionotropic glutamate receptor activity (Enrichment score 3.35)	GO:0005234 GO:0004970 GO:0008066 GO:0005230	2.86E-04 2.86E-04 6.36E-04 0.00745521	*GRIN2A, GRIN3A, GRIN2B, GRIN3B, GRID2*

Supplemental Table 2A. Primers for FPG assays. (Related to Figure 5)

Primers for promoter regions.

Genes	Forward (5' to 3')	Reverse (5' to 3')
b-actin	CCCATCGCCAAAACTCTTCA	GGCCACTCGAGCCATAAAAG
b-globin	TGACCAATAGTCTCGGAGTCCTG	AGGCTGAAGGCCTGTCCTTT
b-tubulin	TCCAGGGATGAAGAATGAGG	TGAGCACTGGTAGGGAGCTT
Arc	CAGCATAAATAGCCGCTGGT	GAGTGTGGCAGGCTCGTC
Bdnf 1	TGATCATCACTCACGACCACG	CAGCCTCTCTGAGCCAGTTACG
Bdnf 2	TGAGGATAGTGGTGGAGTTG	TAACCTTTTCCTCCTCC
Bdnf 4	GCGCGGAATTCTGATTCTGGTAAT	GAGAGGGCTCCACGCTGCCTTGACG
Cdk5	CGCAGCCTGTTGGACTTTGT	GCGTTGCAGAGGAGGTGGTA
GluR1	GGAGGAGAGCAGAGGGAGAG	TTCCTGCAATTCCTTGCTTG
GluR2	GCGGTGCTAAAATCGAATGC	ACAGAGAGGGGCAGGCAG
NR2A	TCGGCTTGGACTGATACGTG	AGGATAGACTGCCCCTGCAC
NR2B	CCTTAGGAAGGGGACGCTTT	GGCAATTAAGGGTTGGGTTC
Svp	CTAGCCTCCCGAATGGAATG	CAGCAGCAGCATCAGCAATG
BNDF-3UTR	CAGTGGCTGGCTCTCTTACC	TGCTGCCATGCATAAAACAT
CamKII	GACCT GGATG CTGAC GAAG	AGGTG ATGGT AGCCA TCCTG
MAP2	CCAGTACCAACAGGGGTTGT	CTCGGGGCTCACAAAGTAAG
SCN2B	TCTGAAATCCACCAACCACA	CCAAGGACCACAAGGTAGGA
SOD1	AGGCTCCTCGGGAACTTTCT	CGGAGCTTTTATAGGCCTGAG
ALSin	TTCACTGAGTCTTCGGTTGC	GGGTGGAGCTAGGCAAGAG
Setx	TCCATTATCGGAGCCTGTTC	TTACCTGCTGGTTCCCTTTG
VAPB	GCGGGAAGAAAGTGGAAGTT	ACGCACGTACGTAGCAGATG
ANG	ACATGGCTCGTTGGTCTAGG	TGTCAGGAAGACCCTGGAAG
TDP43	AGGGACCATTTTGCAGATCA	GTAACGCGGTAGATGGCTTC
FUS	AGTGGGGTAGAGGTGTGTCG	GGGACGTACCAAGTGGAGAA
SMN	GCATCAAGAACCAGCAAACA	CCAACTCACTCCTCCCACAT

Supplemental Table 2B. Primer sequences used in pre-CLIP and CLIP-qRT-PCR to Detect Retention of 5' Splice Junctions of *Bdnf* Exons. (Related to Figure 5)

5' Splice junction @		Sequence (5' to 3')
Exon1/Intron1	Forward	GTGTCTCTCAGAATGAGGGCGTTT
	Reverse	GTGAAGTGCTAGGAAGAGCCATGA

Exon2/Intron2	Forward	TGAAGTTGGCTTCCTAGCGGTGTA
	Reverse	CCCAGGTTCTCACCTAGGTCAATTT
Exon3/Intron3	Forward	TTGGAGGGCTCCTGCTTCTCAA
	Reverse	CATCTTCACTCCCTGCTAGGCTAC
Exon4/Intron4	Forward	ACAGGAGTACATATCGGCCACCAA
	Reverse	CCCGGATAGCATTACACCAAGTTAC
Exon5/Intron5	Forward	GGCAGACGAGAAAGCGCA
	Reverse	CCAAATTTGCGTGGAGAGTGCCTA
Exon6/Intron6	Forward	AACTTGGGACCCTTCTTATCGCTG
	Reverse	TCCTCCTTGGATCCTCCCTCTCT
CDS	Forward	TGTCTCTGCTTCCTTCCCACAGTT
	Reverse	CCGCCTTCATGCAACCGAAGTATG
Rplp0	Forward	CCGATCTGCAGACACACACT
	Reverse	ACCCTGAAGTGCTCGACATC

Supplemental Table 2C. *Bdnf* 5' Splice Junction and 3'UTR Oligoribonucleotides Used in FUS-RNA Electrophoretic Mobility Shift Assays. (Related to Figure 6)

RNA Oligo ID	**Sequence (5' to 3')**
Exon1/Intron1	AAGCCACAAUGGUGAGUAGCAAUA
Exon2/Intron2	GCCGCAAAGAAGGUAAGCACCGGG
Exon3/Intron3	CUUGAGCCCAGGUCCGAGUCAGGC
Exon4/Intron4	GACUGAAAAAGGUGGGUUUCUUUU
Exon5/Intron5	UGGACCCUGAGGUAGGCGACUGCG
Exon6/Intron6	UUUCAUCCGGGAGUAGGUUGGGUGUU
Exon7/Intron7	GUGUCGUAAAGGUGAGCAACAAAG
3’ UTR #1	ACAAUGUCAAGGUGCUGUUGUCAU
3’ UTR #2	CUAGGAUGGAGGUGGGGAAUGGUAC
3’ UTR #3	GACAUAGCAAGGUGCUUUCACUGU
3’ UTR #4	GCUACAUGUUGGUGGUUUAUGUUGA

Qiu, Lee, et al.
Full unedited gel for Figure 2A

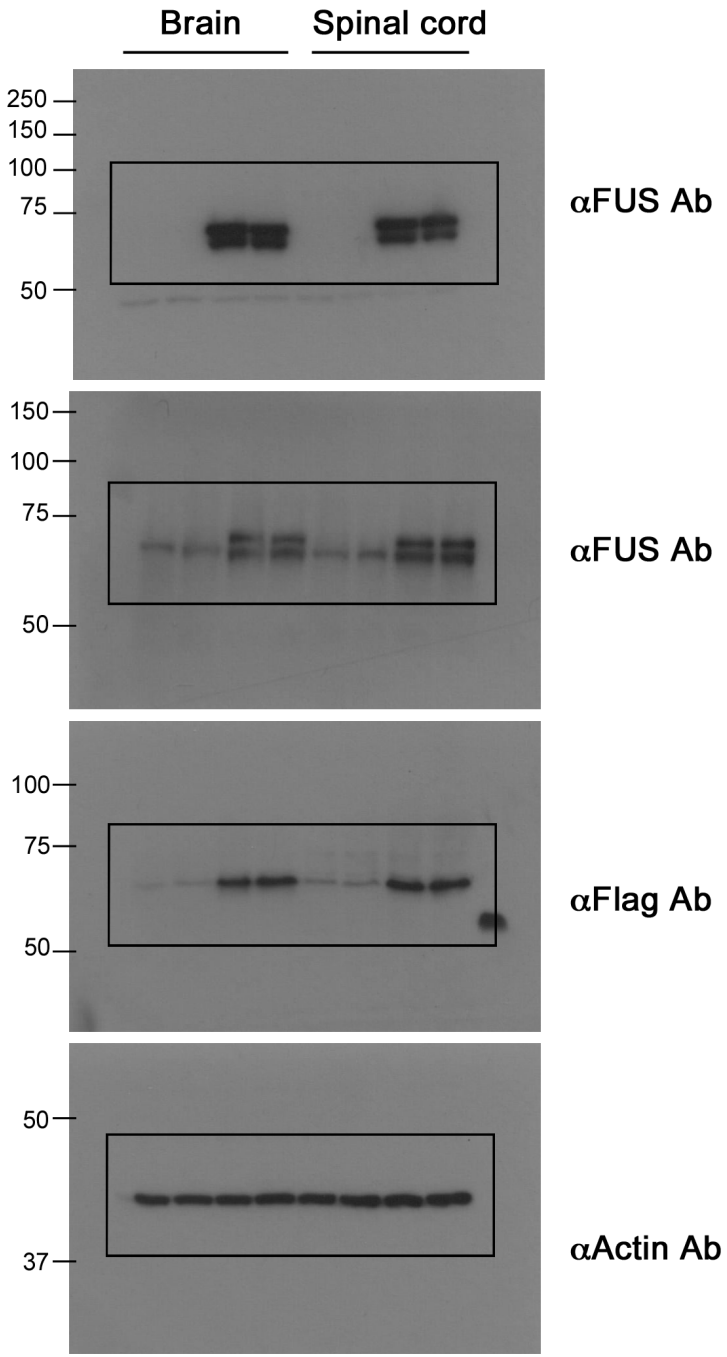

Qiu, Lee, et al.
Full unedited gel for Figure 2C, 2D

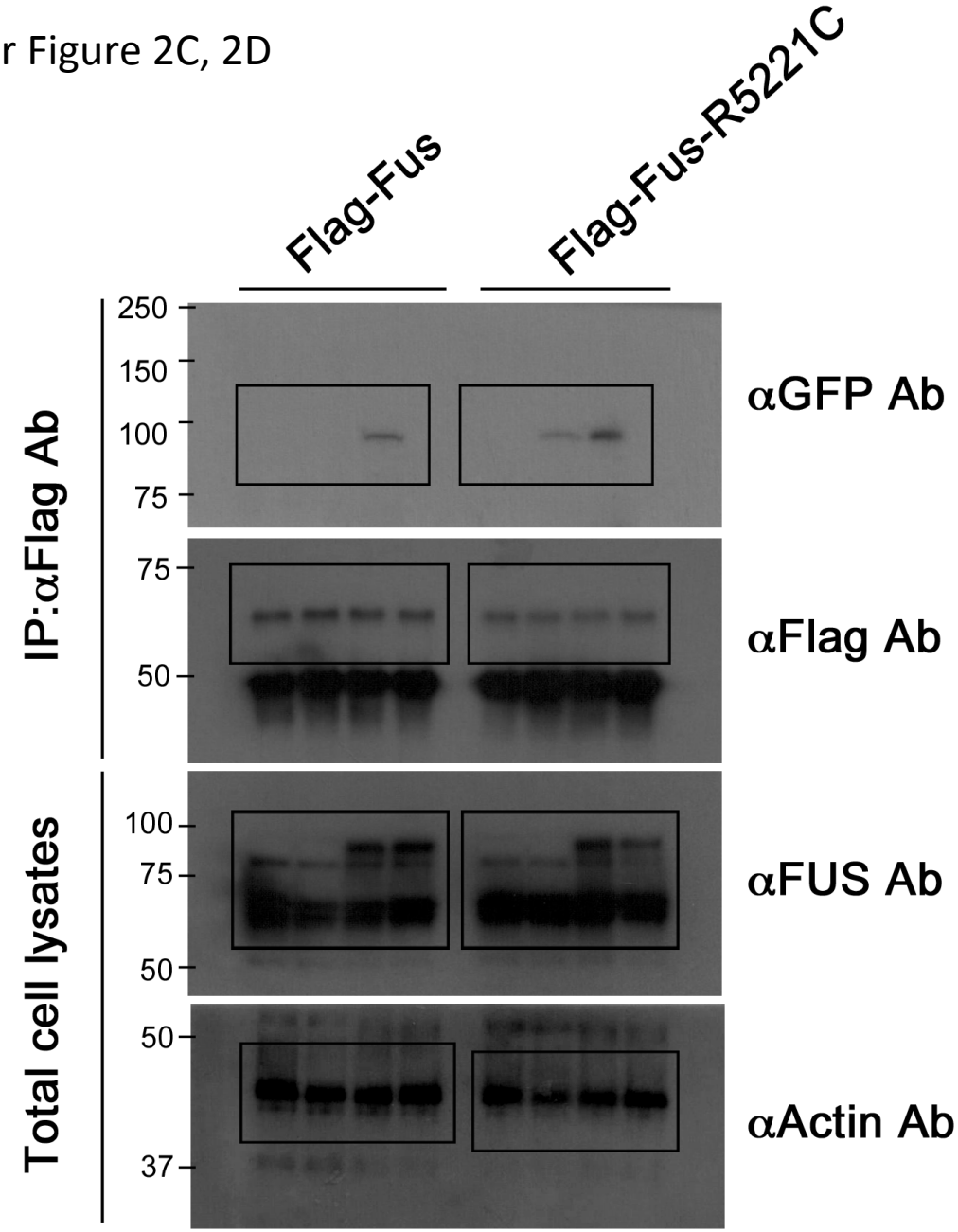

Qiu, Lee, et al.
Full unedited gel for Figure 2E

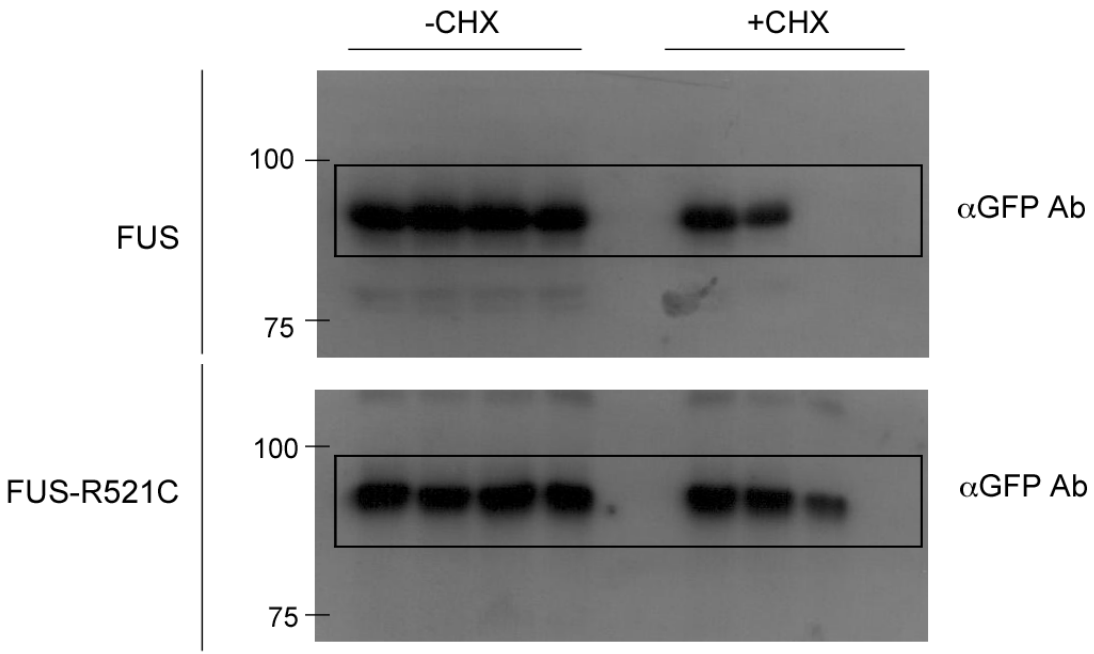

Qiu, Lee, et al.
Full unedited gel for Figure 3A

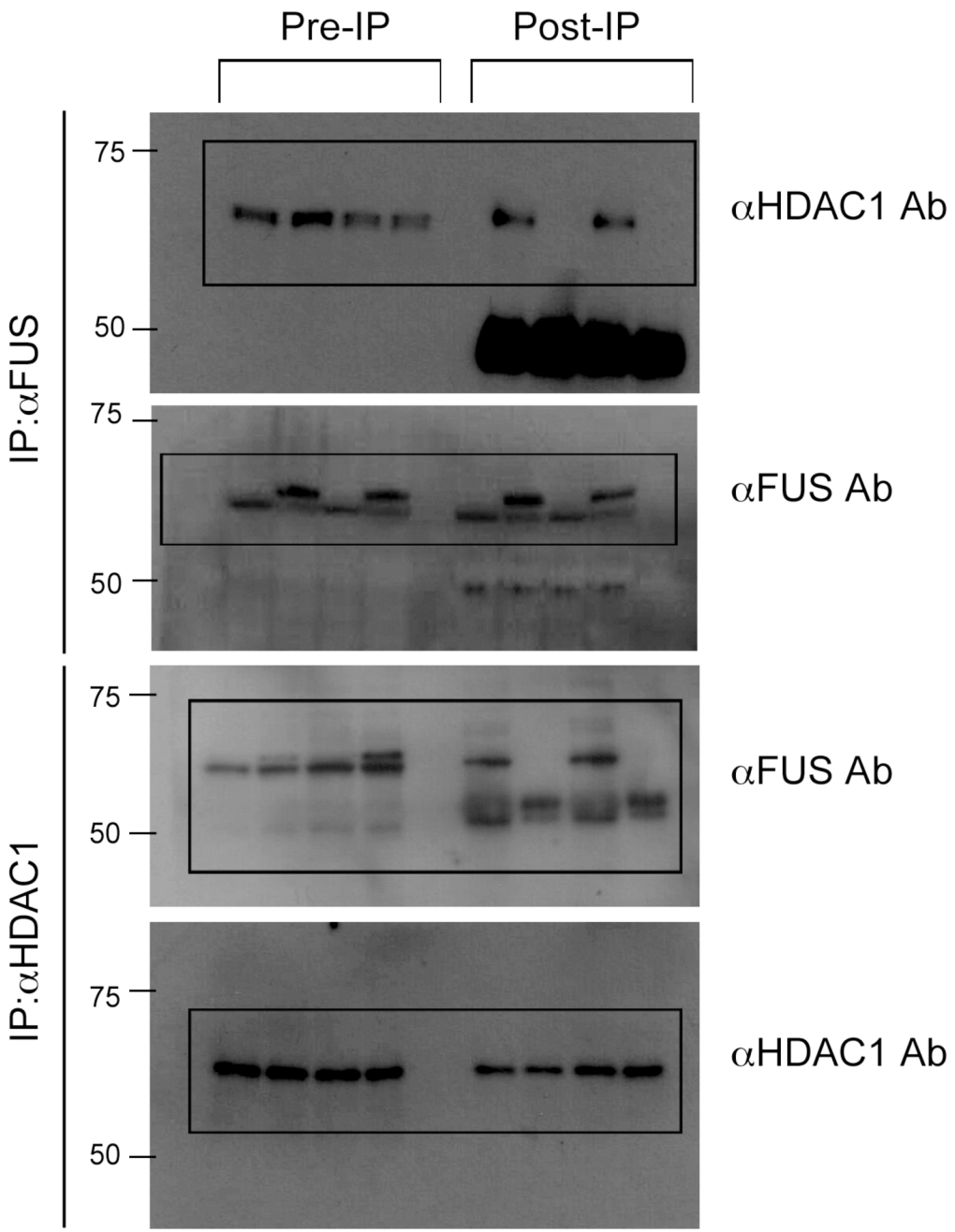

Qiu, Lee, et al.
Full unedited gel for Figure 3B

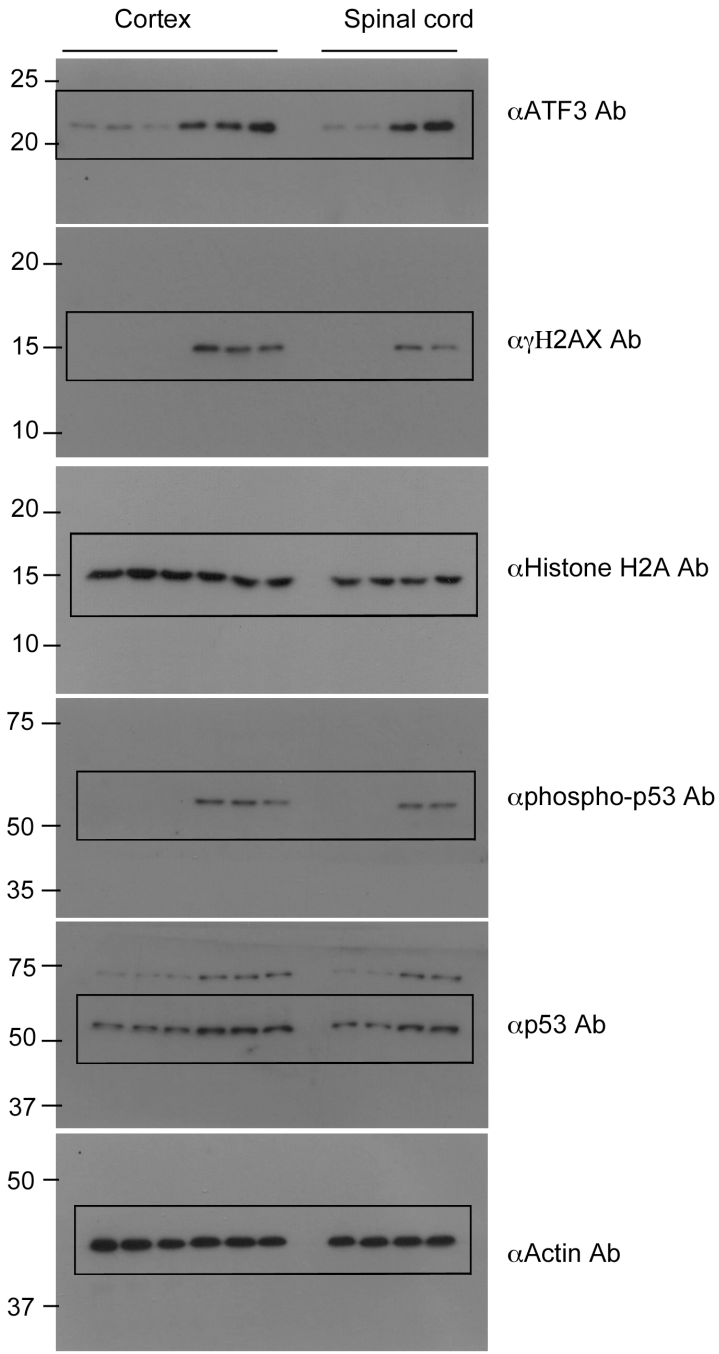

Qiu, Lee, et al.
Full unedited gel for Figure 7A

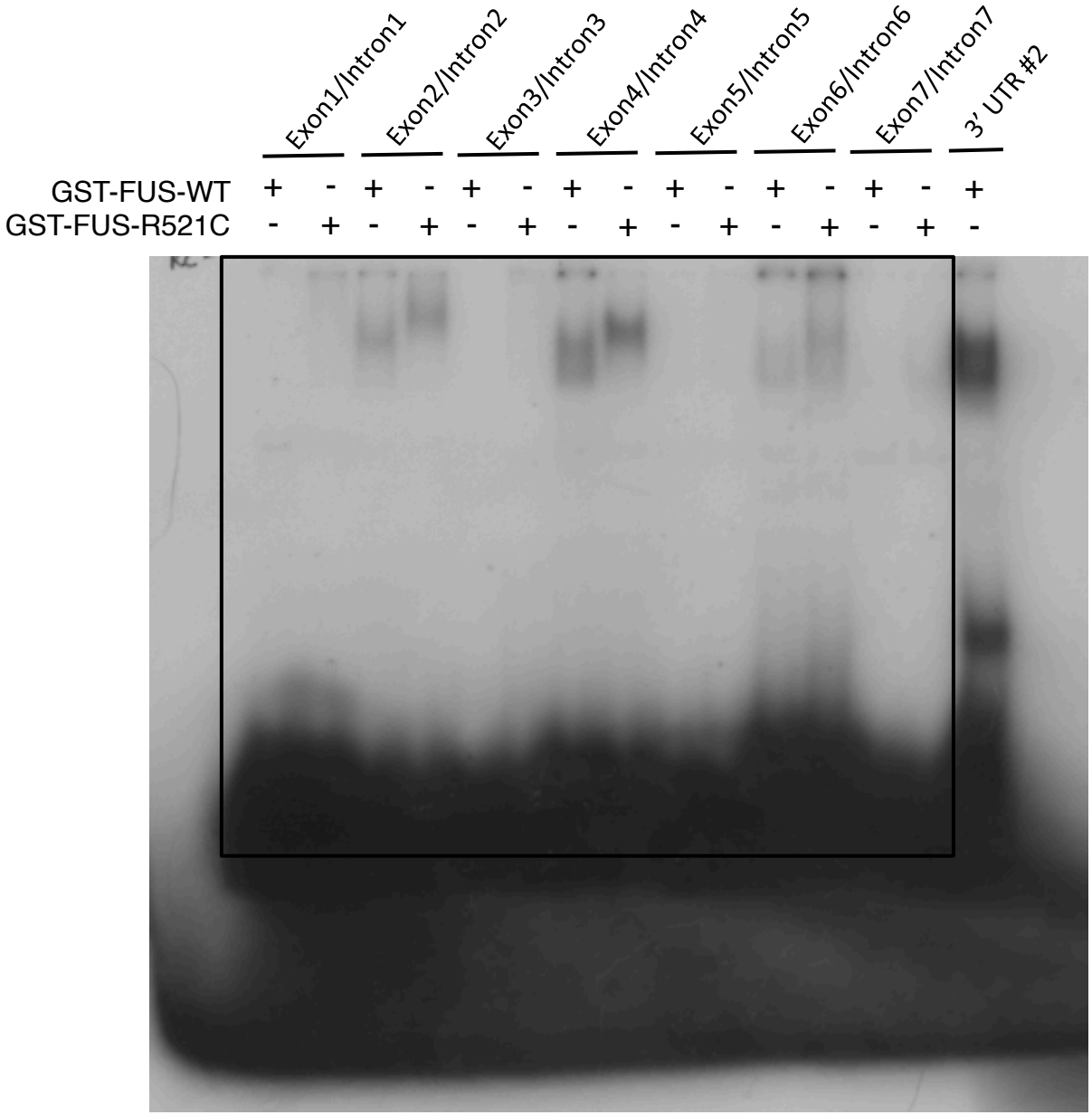

Qiu, Lee, et al.
Full unedited gel for Figure 7B

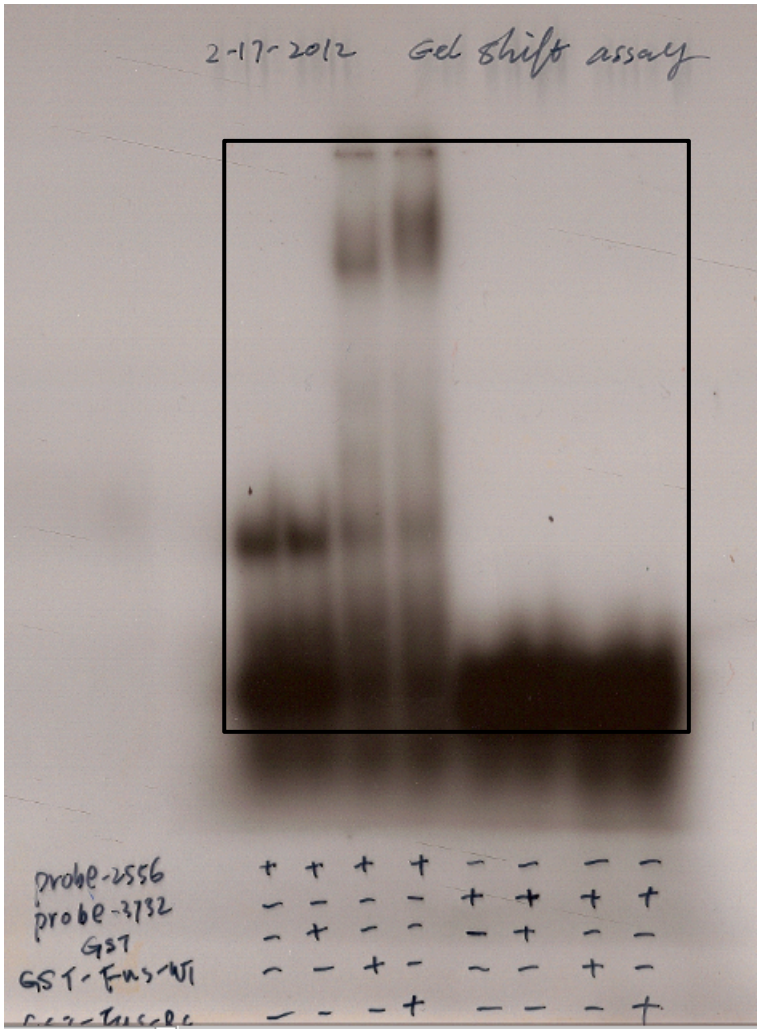

Qiu, Lee, et al.
Full unedited gel for Figure 7C

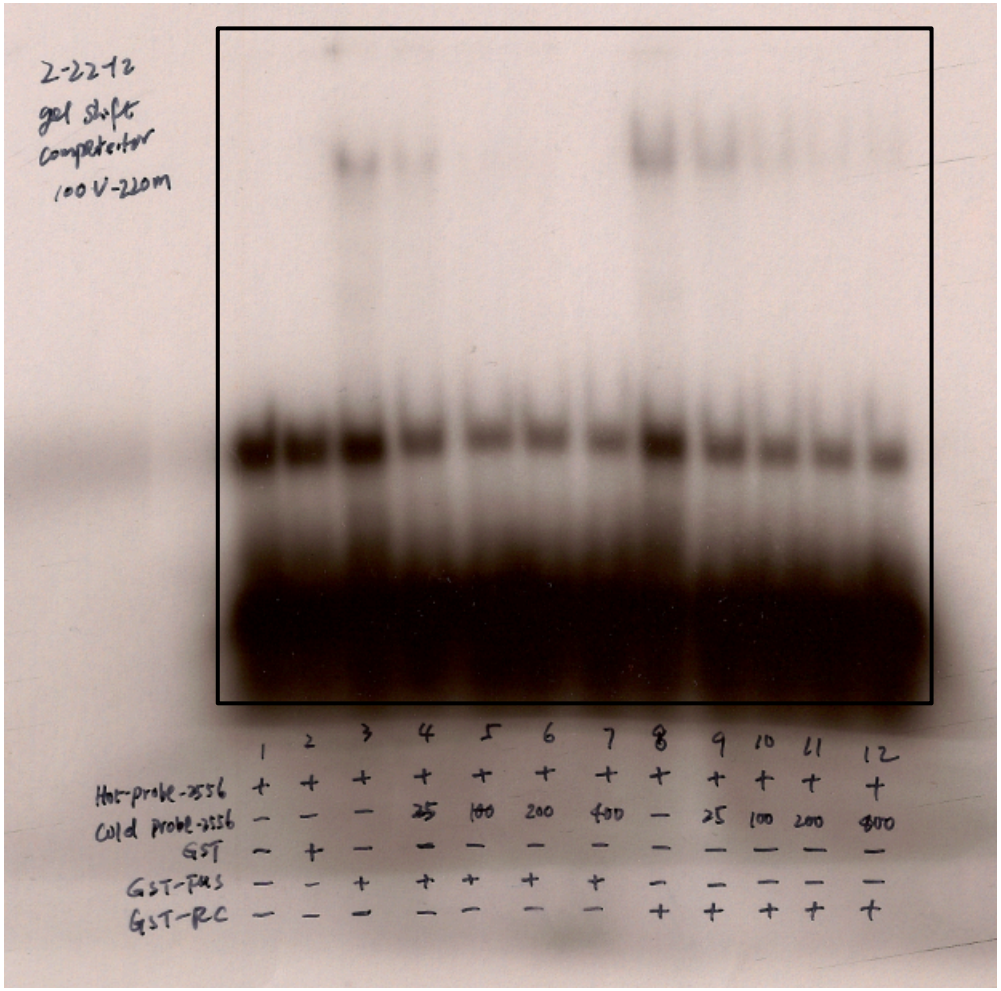

Qiu, Lee, et al.
Full unedited gel for Figure 8B

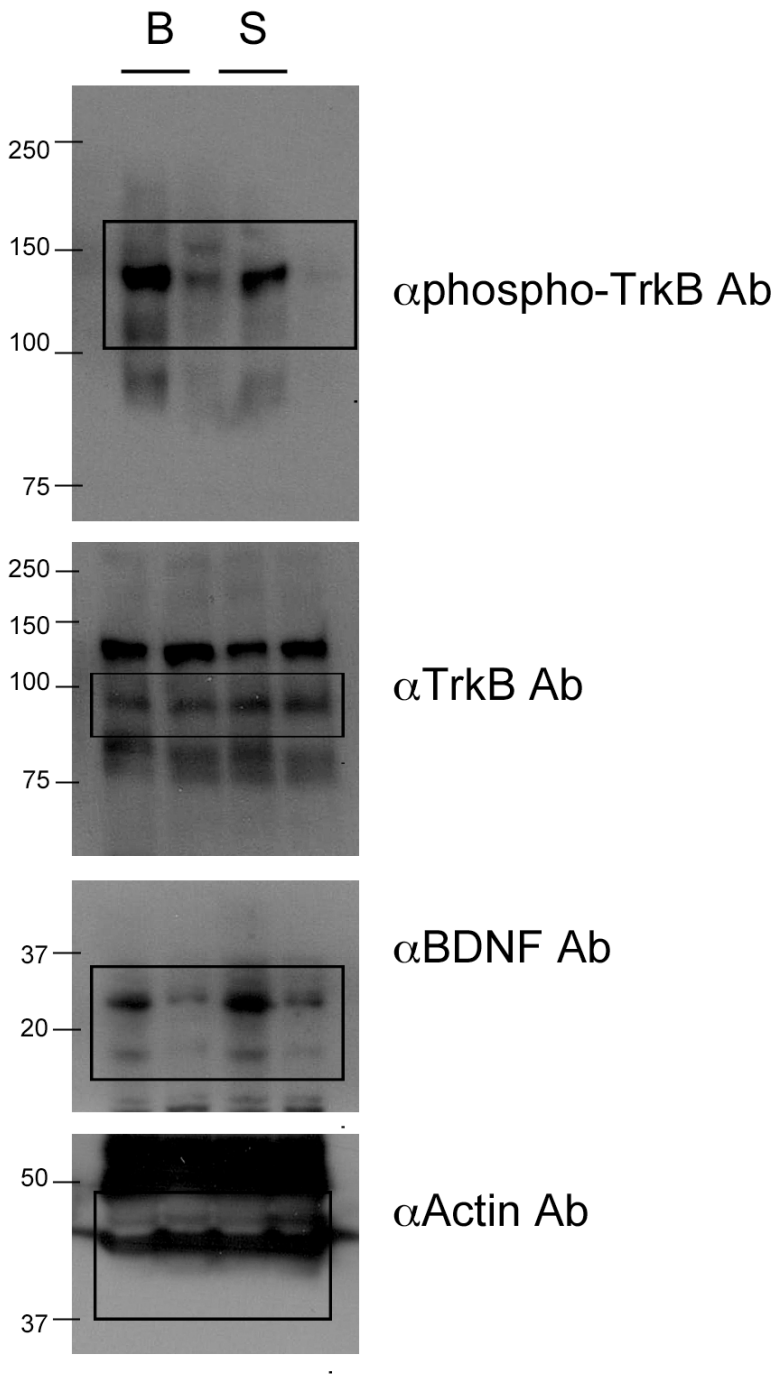

Qiu, Lee, et al.
Full unedited gel for Figure 8E

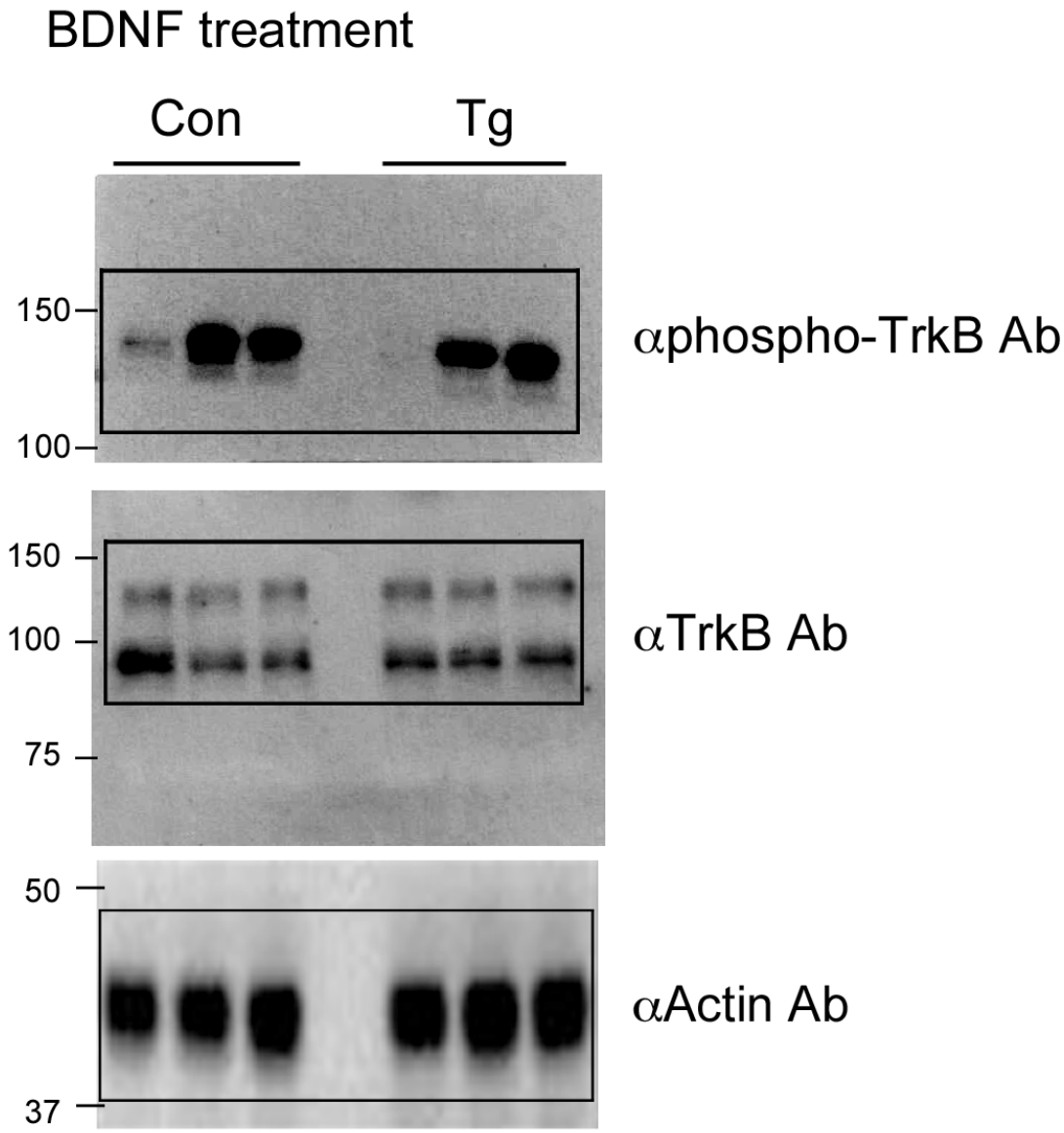

Qiu, Lee, et al.
Full unedited gel for Supplemental Figure 6

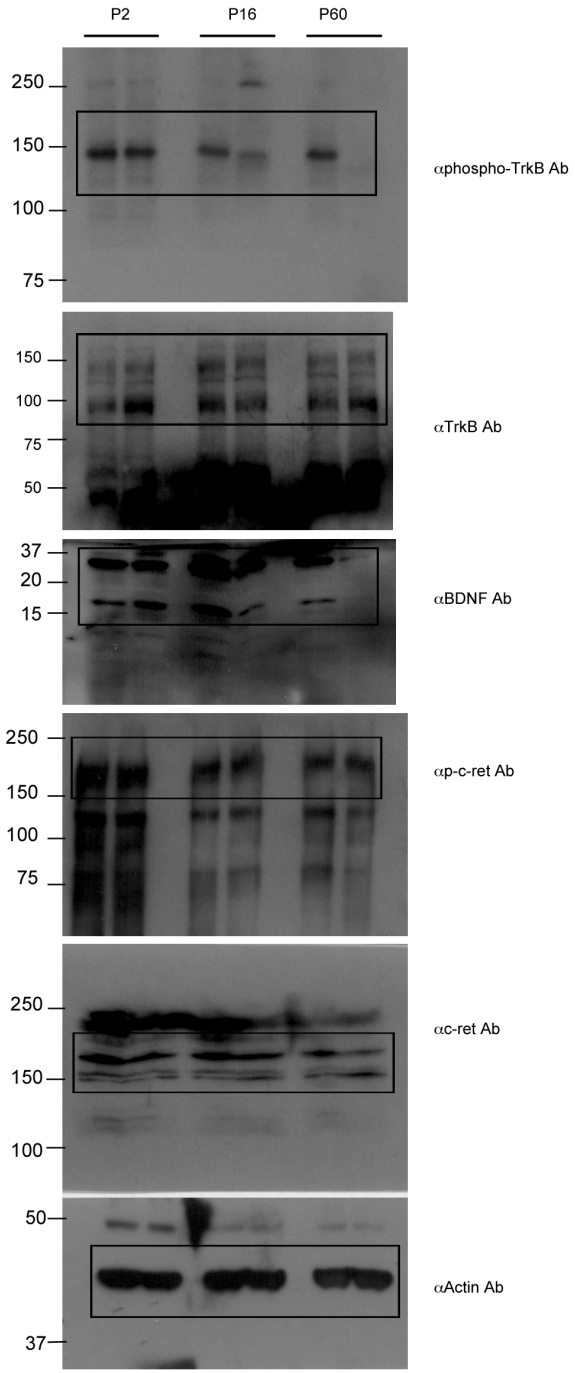

Qiu, Lee, et al.
Full unedited gel for Supplemental Figure 10